Earthquakes and Structures, *Vol. 8, No. 3 (2015) 761-778*
DOI: http://dx.doi.org/10.12989/eas.2015.8.3.761

Seismic improvement of infilled nonductile RC frames with external mesh reinforcement and plaster composite

Mehmet Kamanli[1a], Hasan H. Korkmaz[1b], Alptug Unal[*1], Fatih S. Balik[2c], Fatih Bahadir[2c] and Mustafa T. Cogurcu[1c]

[1]Department of Civil Engineering, Selcuk University Engineering Faculty, Konya, Turkey
[2]Department of Civil Engineering, Necmettin Erbakan University Eregli Kemal Akman High School, Konya, Turkey

(Received December 30, 2013, Revised July 15, 2014, Accepted August 15, 2014)

Abstract. The objective of this paper is to report the result of an experimental program conducted on the strengthening of nonductile RC frames by using external mesh reinforcement and plaster application. The main objective was to test an alternative strengthening technique for reinforced concrete buildings, which could be applied with minimum disturbance to the occupants. Generic specimen is two floors and one bay RC frame in ½ scales. The basic aim of tested strengthening techniques is to upgrade strength, ductility and stiffness of the member and/or the structural system. Six specimens, two of which were reference specimens and the remaining four of which had deficient steel detailing and poor concrete quality were strengthened and tested in an experimental program under cyclic loading. The parameters of the experimental study are mesh reinforcement ratio and plaster thickness of the infilled wall. The effects of the mesh reinforced plaster application for strengthening on behavior, strength, stiffness, failure mode and ductility of the specimens were investigated. Premature and unexpected failure mode has been observed at first and second specimens failed due to inadequate plaster thickness. Also third strengthened specimen failed due to inadequate lap splice of the external mesh reinforcement. The last modified specimen behaved satisfactorily with higher ultimate load carrying capacity. Externally reinforced infill wall composites improve seismic behavior by increasing lateral strength, lateral stiffness, and energy dissipation capacity of reinforced concrete buildings, and limit both structural and nonstructural damages caused by earthquakes.

Keywords: concrete/reinforced concrete; earthquakes; frame-wall system; stiffness degradation; strengthening

1. Introduction

90% of the land area of Turkey is situated on one of the most active seismic zones of the world and devastating earthquakes frequently occur. Structures located in the seismically active zones are far from possessing qualities that would ensure satisfactory seismic performance (Ozcebe *et al.*

*Corresponding author, Research Assistant, E-mail: alptugunal@selcuk.edu.tr
[a]Professor, E-mail: mkamanli@selcuk.edu.tr
[b]Professor
[c]Ph.D.

http://www.techno-press.org/?journal=eas&subpage=7 ISSN: 2092-7614 (Print), 2092-7622 (Online)

2003). A great number of reinforced concrete (RC) structures had totally collapsed or were severely damaged due to recent six major earthquakes causing extensive structural damage and loss of human lives. Most existing concrete buildings in the highly seismic zone comprise nonductile RC beam-column frames and they do not have enough seismic resistance capacity. Seismic behavior was inherent in the structural system and under lateral loading, such as earthquakes, owing to excessive interstory drift. The main reason of this fact is the lack of supervision at the design and construction stages. In collapsed structures several detailing and construction mistakes, such as failures of beam-column connections, spalling of column end regions, buckling of column longitudinal reinforcement, low concrete quality, nonseismic reinforcement details were observed. Also, strong beam-weak column joints are prone to story failures. Widely-spaced ties, irregular designed structural systems, formation of soft stories, short columns are common features (Kara and Altin 2006). Nonductile RC framed structures with those deficiencies comprise a major group among the total building stock. Several studies have been conducted to enhance the seismic performance of nonductile RC framed structures (Blackard *et al.* 2009, Stavridis *et al*. 2012, Baloevic *et al.* 2013).

Longitudinal reinforcement in columns normally was lap-spliced with short length just above the floor level and the yield strength of the longitudinal bars cannot be developed. Joint transverse reinforcement was not common and member ends are not properly confined. Transverse reinforcement generally included hoops with 90-degree bends and those stirrups have wide spacing. Column transverse reinforcements were not exist along the beam-column joints and inadequate confinement at the joints caused formation of plastic hinges that cannot dissipate sufficient energy. Those structures also exhibit inadequate and poor displacement ductility and they have poor stiffness performance under lateral loading as well as inadequate protection against vertical collapse. Some structures were collapsed under their self weight due to insufficient strength. Tragic examples of this collapses are Zumrut Apartment in Konya (2004) with 98 dead and Hicret Apartment in Diyarbakir (1983) with 84 dead. Several similar failures occurred in Turkey and a large number of structures in use have similar characteristics.

Following the 1999 Marmara earthquake in which more than 20000 people died, urgent necessity for improving the seismic resistance of RC framed structures is obvious. Concerns for seismic rehabilitation or strengthening of existing nonductile RC frames are the major concept of the structural engineers. Different strategies can be pursued in the seismic upgrade and repair of existing structures such as, introducing new structural components to the structure or by strengthening existing elements with external jacketing, mechanical attachment of steel *L* shaped profiles placed around the column or beams (Li *et al.* 2002, Karbhari 1993) and use of fiber reinforced plastic (FRP).

Strengthening of individual members becomes not feasible when there are too many members to be rehabilitated and the lateral rigidity of the structure is not adequate (Susoy 2004). To mitigate seismic risks and to improve the lateral rigidity of nonductile frame buildings, the simplest common and effective approaches include addition of an adequate number of structural walls or steel bracings (Nateghi 1995, Pujol and Fick 2010, Ozel and Guneyisi 2011, Uva *et al.* 2012, Massumi and Absalan 2013). Adding new RC shear walls to reinforced concrete frames is a common and reliable method (Anil and Altin 2007). Strengthening of R/C framed structures by using cast-in-place R/C infills leads to a huge construction work and it is necessary to evacuate the building for a few months. This method is questionable as far as the strengthening of a large number of structures is concerned. Thus new Turkish Earthquake Code TEC 2007 presented faster and easier methods, which would not interrupt the use of the building. The lateral load carrying capacity and stiffness of existing structures can be significantly augmented through with the use of existing brick infill walls as shear wall. It is known that, brick infill walls reduce the interstory drift ratio and increase the lateral load carrying capacity of the RC frame. Although the infill increased the strength of the frame, failure was relatively brittle and due to low tensile, shear and compressive strength stiffness contribution to the frame system is limited owing to failure of the existing column lap splices. At this point use of precast panels or use of CFRP over the available infill walls can solve the brittle shear failure of the brick units. Integration and connection of the wall into the existing frame, and transfer of loads to the foundation are important design points. Another proposed strengthening method presented in the TEC 2007 is the use of external mesh reinforcement and plaster over the infills. This method of rehabilitation is expected to be more feasible and not disturbing function of the building and occupants. Since this proposal is new for Turkish engineers and researchers, only few analytical studies exist in the literature (Smyth *et al.* 2004, Guneyisi and Altay 2005, Guneyisi and Altay 2008).

This paper presents the results of an experimental study conducted on the earthquake strengthening of nonductile RC frames. The main concept is to investigate the behavior of the seismic strengthening method by bonding mesh reinforcement with plaster on hollow brick masonry infill walls.

1.1 Research significance

The aim of this research is to convert the infill into a load carrying system acting as a cast-in-place concrete shear wall. The benefit of the method is increase the stiffness of the frames and to improve the seismic performance of poorly constructed RC frames with decreasing the time and the workmanship and minimum disturbance to the occupants. Ghobarah *et al.* (2000) stated that, the earthquake performance of the buildings with poor construction details cannot be satisfactory due to the high value of drift. The proposed method should be convenient in terms of the materials and workmanship so that a huge number of vulnerable buildings can be retrofitted against earthquakes (Susoy 2004).

An investigation of the effect of this technique to lateral strength and stiffness of specimen was necessary for safe and economical strengthening. An important advantage of this technique is that it can be applied without evacuating the building during its application, thus causing minimum disturbance to the occupants (Altin *et al*. 2007).

2. Experimental program

2.1 Test specimens

In current research six specimens were prepared with identical geometric dimensions, reinforcement patterns and materials used. Specimens were tested at Structural Mechanics Laboratory of Selcuk University. The test frame was a 1/2-scale, one-bay, two-storey nonductile RC frame. In order to prevent wrong interpretations of the experimental results, the model ratio was chosen as close to 1/1 as possible. The height of one storey was 1500 mm and length of the specimen was 2360 mm. The columns dimensions were 160×240 mm, the beams dimensions were 240×240 mm. In columns, four 12 mm diameter longitudinal reinforcement and in beams six 12 mm diameter plain bars were used. Plain bars with a diameter of 8 mm spaced at 150 mm were used as ties. Dimensions and reinforcement details of the test frames are given in Fig. 1.

Test frames possessing commonly observed weaknesses in residential buildings in Turkey. Plain bars were used as longitudinal and transverse reinforcement. Such steel has been used in most of the existing buildings. Transverse reinforcements were spaced with 150 mm intervals. Column ends and joint regions were not sufficiently confined. Insufficient lap splices exist at column and beam ends (Figs. 2-3). Also during design phase of the frames, formation of weak-column, strong-beam connections that are encountered frequently in practice were aimed.

In the experimental program totally six specimens were tested. First two specimens (RFB1 and RISPS) contain no strengthening. Specimen 1 (RFB1) was the bare frame with no infill wall and used as reference specimen. The second specimen (RISPS) was also reference specimen with ordinary infill wall. The other specimens were strengthened by introducing external mesh reinforcement and plaster over the existing brick infill wall. The mesh reinforcement was consisted of 16 mm×16 mm square meshes. The diameter of the mesh was ϕ1.1. The yield strength of the mesh reinforcement is 340 MPa and ultimate strength is 420 MPa.

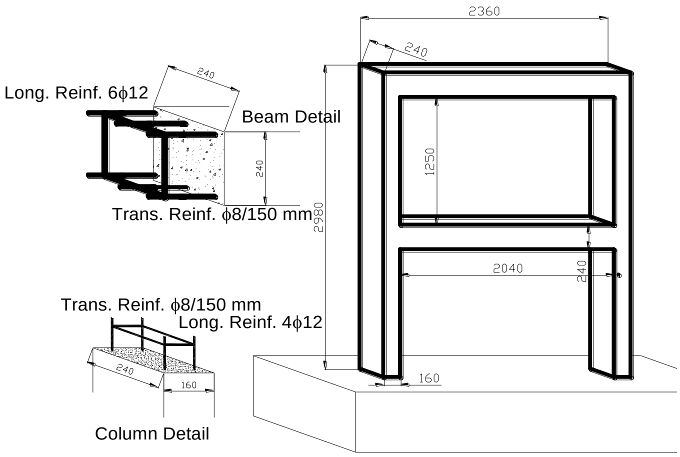

Fig. 1 Dimensions and reinforcement details of the test frames (in mm)

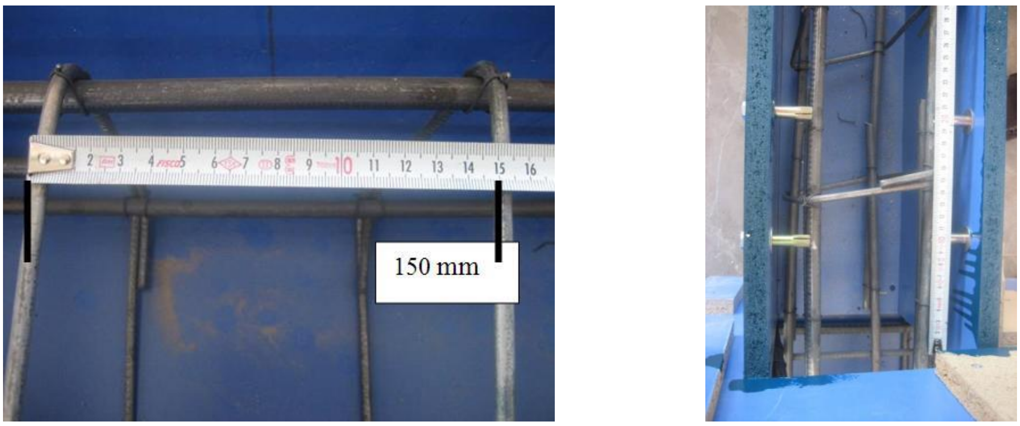

Fig. 2 Stirrups spacing and column end lap splice (Korkmaz *et al*. 2010)

Fig. 3 Reinforcement details of the specimen (Korkmaz *et al*. 2010)

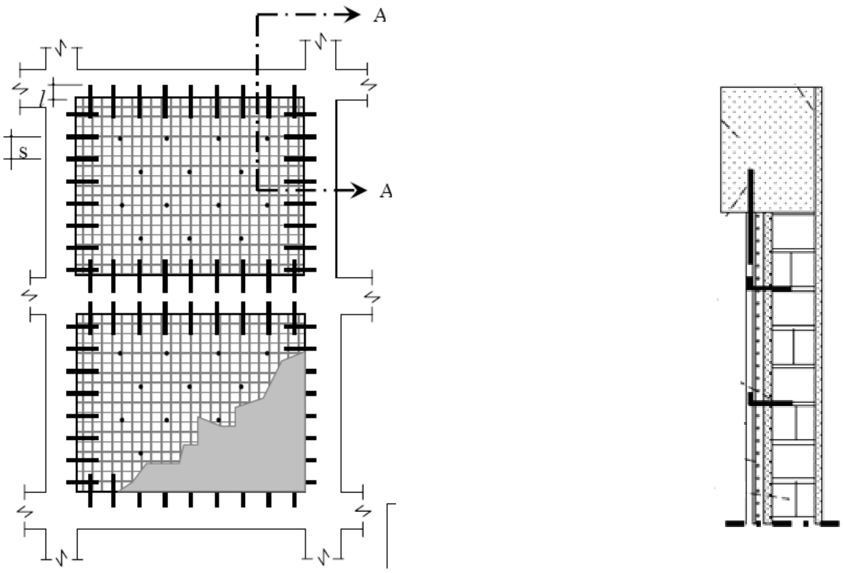

Fig. 4 Plastered wall with welded external mesh and plaster composite (TEC-2007)

The connection between the existing frame and the infill was achieved by means of steel dowels that were made up of 10 mm diameter bars embedded into columns and beams. These dowels were expected to transfer the shear forces from beam to the infill wall. On the inner faces beams and columns, holes were drilled and cleaned with pressured air. The depth of the holes equals to 10ϕ. The external mesh was applied on the inner faces of the wall panels and epoxy was injected in to holes and dowels were inserted into the prepared holes. Finally plaster prepared according to the mix proportion given in the Turkish Earthquake Code is applied on the surface of the mesh-wall composite (Fig. 4).

The static tests were setup in a vertical plane. All the specimens were cast in a horizontal position in the laboratory. The specimens were lifted from the laboratory floor to the vertical position and brick infill walls were constructed. The specimens have the common property of weakly connection between the frames and the infills. Blocks were laid such that their holes were oriented vertically. Special ½ scaled perforated clay bricks were used. For strengthened specimens first dowel holes were drilled and mesh reinforcement placed, finally dowels were anchored. At the last stage plaster was applied on the surface of the wall-mesh interface. Specimens were tested after the plaster has gained strength.

The joint mortar, made of cement, lime, and sand in the proportion 1.0:0.65:6.6 was used to construct the brick masonry wall. Frames with low compressive strength were constructed. 15 MPa concrete compressive strength was aimed to represent the concrete strength of the existing buildings in Turkey.

2.2 Instrumentation and test procedure

The testing system consisted of strong floor, reaction wall, loading equipment, instrumentation, and data acquisition system. A steel stability frame was constructed around the test specimen in order to prevent out-of-plane movements. The specimens were built on stiff reinforced concrete base foundation and this was anchored to the laboratory's strong floor by high-strength steel bolts. The lateral loads were imposed by means of hydraulic actuators placed against a rigid reaction wall. Specimens were tested under cyclic lateral loading applied to both stories at beam levels. A special loading apparatus was used to apply 1/3 of the base shear to the first story and 2/3 of the base shear to the second story. The ratio of the top storey load to the middle storey load was 2. Magnitude of the total force was measured by a load cell with 50 ton compression and 30 ton tension capacities. The schematic representation of test setup, loading system, and instrumentation is shown in Fig. 5.

The axial load to simulate a dead load was applied to the specimen columns by two vertical hydraulic jacks. Approximately 15% of the axial load capacity of the columns was applied to the columns top prior to testing the specimen. Reversed cyclic lateral loading scheme is applied in order to represent the earthquake loading. Two categories of loading were considered, i.e., service level loading and ultimate loading. First cycle is the load targeted elastic cycle and finalized before the predicted yield load. After yield limit of the specimen, displacements targeted or based cycles were applied. Reversed cycles are applied to determine the yield point and complete shape of the load-displacement curve.

The specimens were instrumented with linear variable differential transformers (LVDT) at strategic locations to measure displacements. During the test, the first and second storey displacements and the lateral loads were measured and monitored. Also load distributions on the storey's were controlled during the testing. At the peak load level of each half-cycle, cracks were

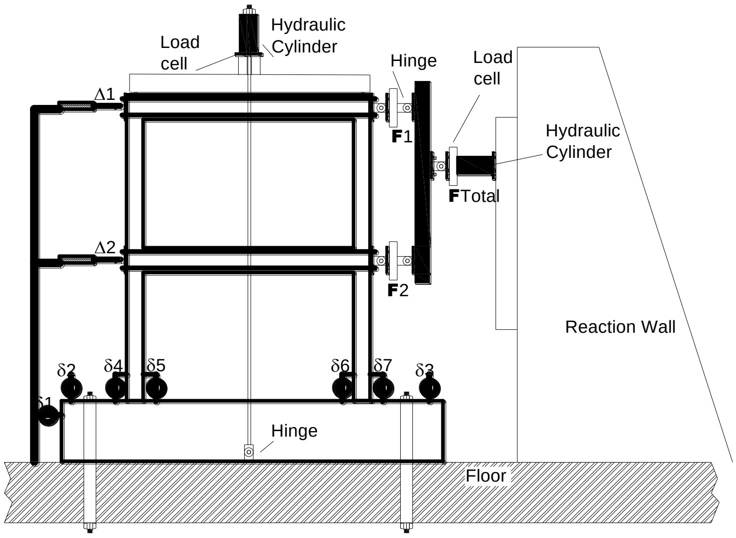

Fig. 5 Test setup, loading system, and instrumentation (Korkmaz *et al*. 2010)

marked on the specimens and the mechanism of failure was observed during testing. To ensure minimum rigid body motion or rotation during the tests, foundation of the specimen was also monitored with three LVDT.

In Fig. 5, Δ_1 and Δ_2 were the top storey and middle storey displacements, respectively. δ_2 was the measurement taken to calculate rigid body motion of the foundation. δ_3 and δ_4 were taken to calculate rigid body rotation of the foundation. L_2 is the distance between the dial gauges δ_3 and δ_4. L_1 is the height of the measurement Δ_1, while $L_1/2$ is the height of the measurement Δ_2 from the bottom of the foundation. The correction factor for Δ_1 can be given by Eq. (1) and the correction factor for Δ_2 can be given by Eq. (2).

$$\eta_1 = \frac{(\delta_1 + \delta_3)}{2} \frac{L_1}{L_2} \tag{1}$$

$$\eta_2 = \frac{(\delta_1 + \delta_3)}{2} \frac{L_1}{2L_2} \tag{2}$$

The net top and middle storey displacements can be written with Eqs. (3) and (4) respectively.

$$T_1 = (\Delta_1 - \delta_2) - \eta_1 \tag{3}$$

$$T_2 = (\Delta_2 - \delta_2) - \eta_2 \tag{4}$$

2.3 Tests summary

Specimen 1 was the reference specimen and contained no infill. The reinforcement details of the specimens were not in accordance to the Turkish Earthquake Code and a nonductile frame was tried to form. RFB1 was tested to understand the bare frame capacity. The representation of the first specimen RFB1 is given in Fig. 6.

Second specimen (RISPS) tested was the reference specimen with unreinforced infill wall. This specimen contained no strengthening and tested to understand the reference behavior of the infilled original frame. The reinforcement details and the quality of the concrete were same as the RFB1. An ordinary brick layer was hired to construct the brick masonry infill wall. Special ½ scaled perforated clay bricks were used with ordinary mortar. Bricks were laid such that their holes were parallel to the horizontal plane (Fig. 7). This application is common in Turkey for external walls of the framed structures. The infill walls were not constructed on the symmetry axis of the frame for simulating exterior walls of the building.

The failure mode of the infill wall was the corner damage and crushing of the wall panel. Bottom storey wall panel damaged more than the upper one. After the infill was crushed at the upper corners due to diagonal compression, the specimen lost its lateral load carrying capacity and thus, failed. The representation of the failure mode of the wall is given in Fig. 8.

Fig. 6 Reference empty frame RFB1 (Korkmaz *et al*. 2010)

Fig. 7 ½ scaled bricks were used with ordinary mortar

Fig. 8 Failure modes of the wall portions (Korkmaz *et al*. 2010)

The third specimen, SPS1, was similar to the specimen RISPS2 and strengthening procedure is applied. Wall construction details were same as the RISPS2. After the infill wall was constructed, holes were drilled on the inner faces of the beams and columns. Since the thickness of the columns was higher than the thickness of the wall, there was enough distance on the face of the beams and columns. After the placement of the mesh reinforcement, holes were filled with epoxy and dowels were inserted. Finally plaster was applied over the surface. The thickness of the plaster was 15 mm.

During testing, specimen SPS1 was showed higher initial stiffness than the RFB1 and RISPS2. Also total lateral load carrying capacity of the SPS1 was increased as compared to SPS1 and RISPS2. Several flexural cracks were observed on the beams and columns. But below the first storey beam, premature and sudden failure of the wall-plaster-dowel interface was observed. The plaster cover over the dowels disintegrated and no more shear transfer between beam and the wall become possible. This failure mode was very sudden and in brittle nature. The full capacity of the mesh-plaster-wall composite couldn't used due to this premature failure. After the failure, the specimen showed similar load-displacement characteristics with the RFB2 specimen. This failure was attributed to inadequate plaster thickness and at the end of the test, it is decided to increase the thickness of the plaster. The failure mode of the specimen at the end of the test is given in Fig. 9. This specimen lost 55% of its lateral load carrying capacity immediately after failure of the dowel anchorage with the mesh plaster composite.

The fourth specimen SP2 was strengthened using the results of the specimen SPS1. The thickness of the plaster was increased and applied as 20 mm. Increase in the plaster thickness in specimen SP2 improved stiffness as compared with Specimen SPS1. This specimen showed higher ultimate load than the specimen SPS1. Again initial flexural cracks were observed on RC members. Specimens SP2, SPS1 showed similar behavior and failure modes. The first cracks over

Fig. 9 Failure mode of specimen SP1 (Korkmaz *et al*. 2010)

Fig. 10 Failure mode of the specimen SP2

the infill observed on the dowels. A similar but more slow type of failure was observed like SPS1. As the applied cycles and displacements increased, disintegration between dowels and plaster become serious. This disintegration dropped the lateral load capacity of the frame. The initial cracks and final failure mode of the specimen is given in Fig. 10.

For specimen SP3, plaster thickness was chosen as 30 mm and also the strength of the plaster was increased to 30 MPa. Since the dimensions of the mesh were smaller than the dimensions of the brick area, two pieces of mesh were applied over the brick wall. The splice line was on the middle of the beam. Two meshes were spliced 300 mm at the junction point.

Flexural cracks initiated and concentrated at column lap splice regions. During the testing, again several cracks were observed on the dowel points but no shear failure was occurred. Instead, the splice of the mesh reinforcement line on the middle was torn. The success of proposed strengthening method mainly depended on the connection provided between the frame and the infill.

The load carrying capacity of the specimen dropped after the failure was observed. This type of

Fig. 11 Failure mode of the specimen SP3

Fig. 12 Failure mode of the specimen SP4

failure progressed more slowly than the failure observed in specimens SPS1 and SP2. The test photos of the SP3 are given in Fig. 11.

After obtaining a splice failure in SP3, and shear failures in SPS1 and SP2, the mesh reinforcement layers of the SP4 was doubled. The plaster thickness was same with SP3. The other RC frame details were identical in all specimens.

Combined type of failure mode in SP4 was observed. Bond deterioration between dowels and the plaster was initiated but not progressed further. Corner crushing of the wall panels were observed especially on the bottom panel. Inclined shear cracks were initiated and they were spreaded over the walls. Ultimate load capacity of the SP4 was noticeably higher than the other specimens. The cracks over the plastered mesh panels showed a load distribution or load sharing between the wall and frame system. The failure mode of the specimen SP4 is given in Fig. 12.

3. Experimental results

The comparison of the behavior of test specimens is made in terms of failure modes, lateral strength, stiffness and energy absorption capacities. The total load applied- lateral displacement hysteresis curves are represented in Fig. 13 for all specimens. In specimen SP2, sudden failure of the dowel-wall interface was clearly observed from the strength drop of load-displacement hysteresis curve in the last cycle. In the last cycle, there is a sudden drop in the load carried by the system and at the same time there is a sudden increase in the lateral displacement. Same type of drop in the lateral load capacity is seen in curves of the SP3 which was failed due to dowel-wall anchorage deterioration too. SPS1 showed inferior behavior among the strengthened specimens.

The torn point of the mesh splice in specimen SP3 and corresponding drop in the lateral load curve is also obvious in Fig. 13(e).

To evaluate and compare the lateral strength and the stiffness of the test specimens, envelope curves were constructed. Those envelope curves were obtained by connecting the peak points of the each load cycle. Response envelope curves of the strengthened specimens are given in Fig. 14 together with the response envelope curve of the reference bare frame and reference specimen RISPS2 to illustrate the effect of applied rehabilitation techniques on the lateral strength, initial stiffness and the drift ratio on the maximum load. The strength envelopes are used for determining general behaviors and strengths of specimens.

Strength and stiffness of both strengthened frames were significantly higher than those of the bare frame. It is obvious that infilled frame higher initial stiffness than the bare frame but strength loss is observed beyond the peak point. The addition of infill walls increased strength and stiffness of nonductile RC frames, and decreased drift ratios, as expected.

Specimen SPS1 and SP2 survived higher lateral loads. The specimen SPS1 approximately followed the infilled specimens (RSPS2) envelope curve and after failure, the load carried by the system was dropped to bare frames level. Specimen SP2 was showed higher performance in terms of lateral load capacity with respect to the SPS1, but sharp decrease in the curve after 15 mm lateral displacement levels is noticeable.

Performance of specimen SP3 is superior to SP2. The load capacity is limited due to anchorage loss of the mesh reinforcement and in specimen SP4, the mesh reinforcement was doubled and lap splice of the mesh pieces were increased. Although several cracks were formed on the anchorage dowels and damage or crushing of the corners of the walls were observed, load carried by the system didn’t dropped rapidly and formation of tensile cracks were observed over the strengthened wall panels.

The ratio of the ultimate lateral strength of Specimens that were strengthened to that of the reference specimen is illustrated in Fig. 15 and ranged between 1.42 and 2.

Stiffness values and stiffness degradation of the specimens were calculated from the load-displacement hysteresis curves for each cycles and presented in Fig. 16. The vertical axes of the Fig. represents the stiffness values in KN/mm scale, while horizontal axes represents the displacement value in mm, at which the stiffness is calculated.

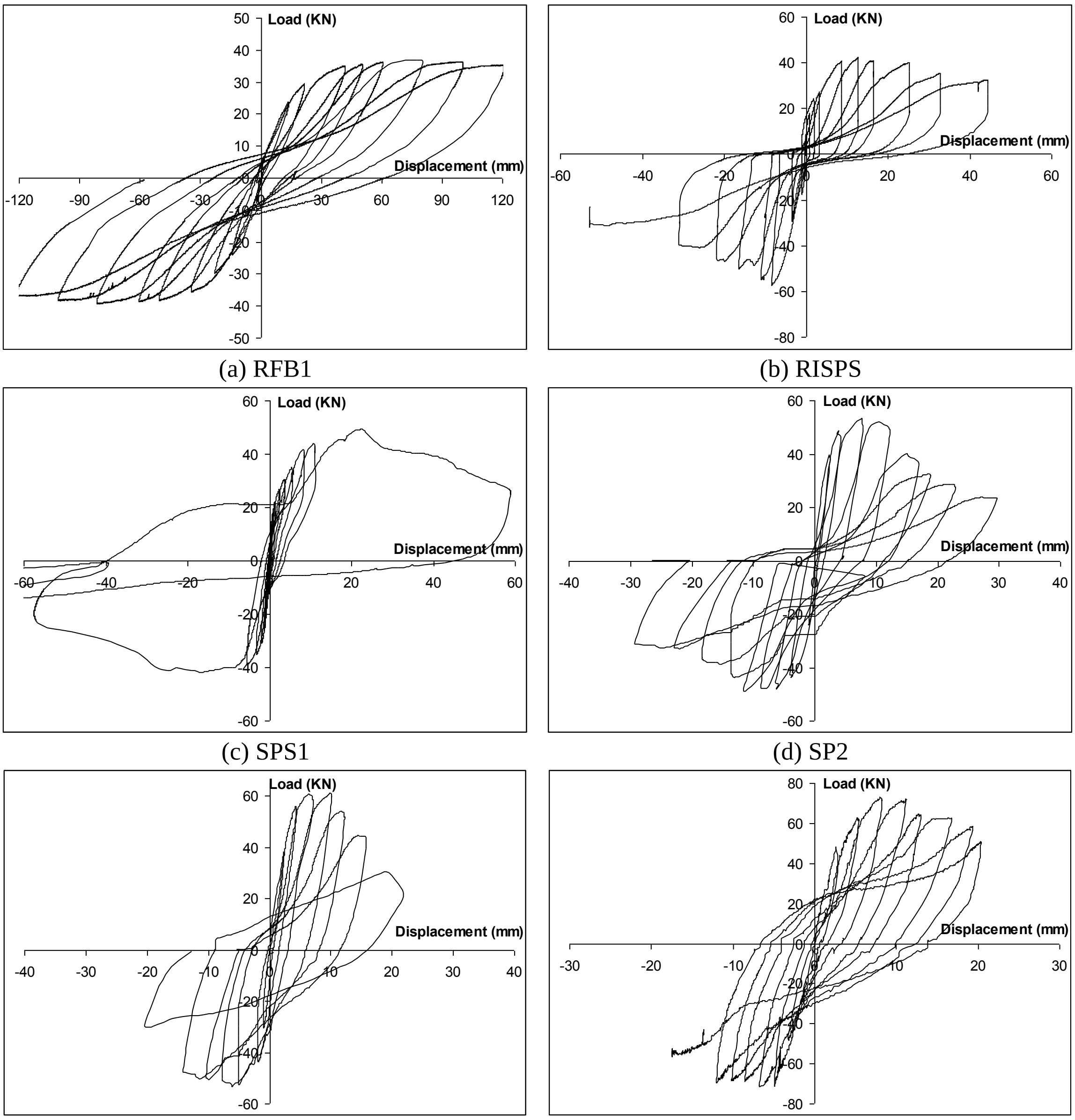

(a) RFB1 (b) RISPS

(c) SPS1 (d) SP2

(e) SP3 (f) SP4

Fig. 13 Load-displacement Hysteretic curves

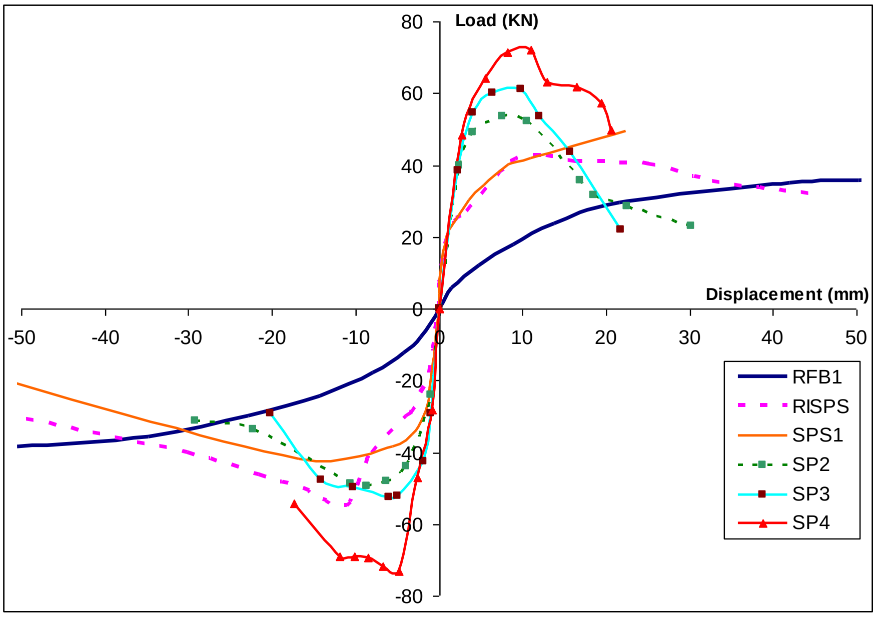

Fig. 14 Envelope curves extracted from the hysteretic curves of the load-displacement curves

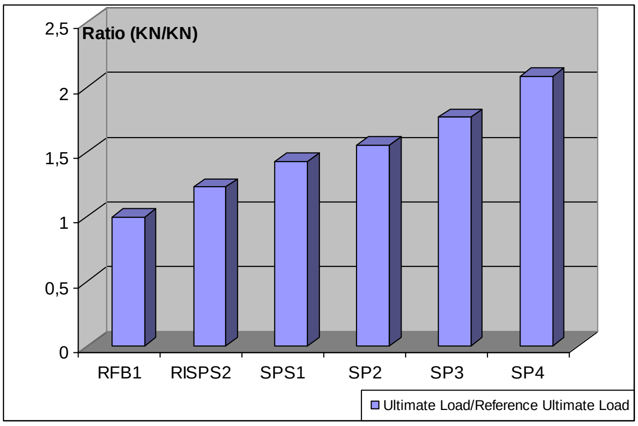

Fig. 15 Ratio of specimen ultimate load to the reference empty specimen's ultimate load

As can be seen from these curves, adding infill walls into the bare frame, and increased strength, stiffness and energy dissipation capacity significantly.

As expected bare frame displayed lowest initial stiffness value among the others. Inclusion of the infill wall increased the stiffness and strength of the frame and decreased the story drift. Initial stiffness value of the specimen SPS1 is close to RISPS2. SP4 displayed highest stiffness values among the other specimens. Stiffness characteristics of the SP3 are superior to the specimens SP2 values. Stiffness degradation is more pronounced for specimens SP2 and SP3 than SP4. As the cycles were applied and the total displacements were increased, stiffness values were decreased. Increasing the stiffness of the structure may prevent early collapse and reduce interstory drift. High

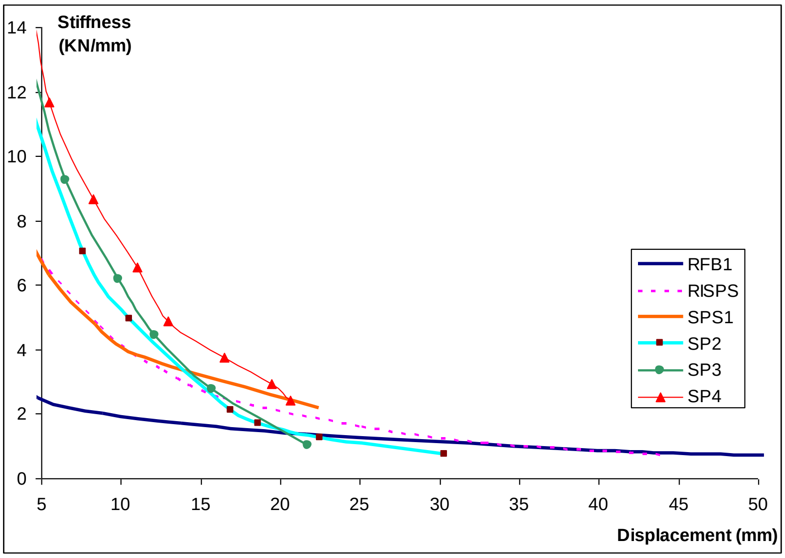

Fig. 16 Stiffness degradation curves of the specimens

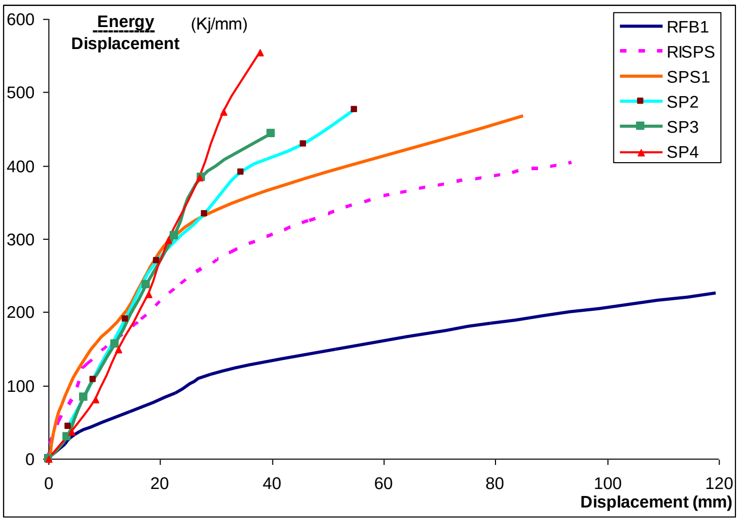

Fig. 17 Depicts the variation of cumulative dissipated energy

drift levels may cause excessive damage to nonstructural elements (Ghobarah *et al.* 2000).

Energy consumption values of the specimens are important for earthquake types of loading point of view. The energy input to the frame system due to quake motion must be dissipated through the frame system. High the energy consumption capacity is the indication of the correct improvement in the system due to strengthening method. The energy absorbed in the loading part is the area under the load-displacement curve. During the unloading stage, some amount of this absorbed energy is recovered. The difference between the absorbed and recovered energy is equal to dissipated energy. The curves of dissipated energy versus cycles are not meaningful for comparison purposes since, in each cycles the final displacement values reached were different and energy values depend on the displacement values. For that reason energy absorption values of the cycles were divided to the corresponding cycle peak displacement. Fig. 17 depicts the variation of cumulative dissipated energy in KJ divided to cycle displacements in mm as a function of peak cycle displacement in mm.

Specimen RFB1, SPS1 and SP2 dissipated the smallest amount of energy among the infilled specimens. The energy dissipation capacity of infilled specimens was significantly improved by the increase in the thickness of plaster.

The behavior of the test specimens in terms of the energy absorption capacities can supply valuable information about the specimens. At this point SP4 showed higher performance. Following the SP4, SP3 displayed superior performance than SP2 and SPS1. Performance of SPS1 and SP2 can be categorized as unsatisfactorily.

4. Conclusions

The results of cyclic tests performed on an RC structure strengthened with mesh reinforcement and plaster have been discussed in the paper. The study was an initial step to cease experimental data shortage and adding valuable experimental test data to literature about the behavior of strengthened masonry infilled RC frames with external mesh reinforcement and plaster composite.

A first aspect to be examined is the behavior of the bare frame compared with the infilled frame case. A comparison can be realized examining the envelope diagrams. The principle difference between the bare frame and frame infilled with unreinforced masonry wall is that the high initial stiffness and high lateral load capacity. Strength, stiffness and energy dissipation capacity of infilled specimen were significantly higher than those for bare frames.

Observing the force-displacement envelopes, panel with external reinforcement collaborates with the frame and it gives non-negligible contribution of strength and stiffness. Panels provide relevant resistance to the lateral loads. Similar results were deduced in the study of Calvi (2000). On the other hand, dowels used as shear keys were debonded at the ultimate load levels of the specimens SPS1. In specimen SP2, the thickness of the plaster is increased and rapid failure of the dowels were delayed but couldn't prevented. The performance of retrofitted frames limited by the premature failure of dowel-plaster-wall interface. As a result, expected performance cannot be obtained from strengthening with composite infill walls.

Thickness increase in specimen SP3 showed significant improvements in strength, stiffness and energy dissipation capacity relative to SPS1 and SP2. Results from specimen SP3 test show that the proposed composites with 30 mm plaster thickness application provide more robust connection and can successfully enhance the original structure. But in this case another failure mode was observed and the external mesh reinforcement suffered anchorage problem.

In specimen SP4 where the anchorage length of the external reinforcement was increased, debonding of the shear keys initiated but didn't progress further. No anchorage problems were encountered for external reinforcement. Instead, infill wall joints were crushed at the upper and lower corners of the infill wall. Also cracks were spread over the reinforced wall panels. Specimen SP4 exhibited significantly higher ultimate strength and higher stiffness than the others.

The maximum drift (Δmax) was approximated as the drift ratio corresponding to the strength deteriorated by 20% of Vmax (0.8 times Vmax) (Han and Jee 2005). Turkish seismic code specifies the interstorey drift limit as 0.35% for the RC framed systems (TEC 2007). This value in Eurocode 8 regulations, for brittle nonstructural infills in contact with the RC frame, is taken equal to 0.5% (Altin *et al.* 2007). For specimen RISPS2 and SPS1, maximum drift ratios were 1.99 and 1.31 respectively. For SP2, SP3 and SP4, Eurocode 8 limit didn't exceeded. There was no significant degradation in lateral load carrying capacity for those specimens up to this limit value.

The authors concluded that, when the external mesh reinforcement-plaster composite were connected correctly with the frames as well as infill wall, new lateral load carrying system was generated, the ultimate lateral load carrying capacity was increased and storey drift ratio was reduced significantly. This technique is an economical, efficient and practical solution for the strengthening for buildings with poor seismic performance.

Acknowledgements

This study was a part of the research project supported by the Selcuk University Scienctific Research Project Office (BAP). The Authors also wishes to thank Dr. Serra Zerrin Korkmaz and Dr. Sami Donduren for the test results of the first two reference specimens and the third specimen and also their support during the study.

References

Altin, S., Anil, O., Kara, M.E. and Kaya, M. (2007), "An experimental study on strengthening of masonry infilled RC frames using diagonal CFRP strips", *Compos. Part B*, **39**, 680-693.

Anil, O. and Altin, S. (2007), "An experimental study on reinforced concrete partially infilled frames", *Eng. Struct.*, **29**, 449-460.

Baloević, G., Radnić, J. and Harapin, A. (2013), "Numerical dynamic tests of masonry-infilled RC frames", *Eng. Struct.*, **50**, 43-55.

Blackard, B., Willam, K. and Mettupalayam, S. (2009), "Experimental observations of masonry infilled RC frames with openings", *ACI SP 265-9, Am. Conc. Inst.*, 199-222.

CEN. EN 1998-1 (2004), *Eurocode 8: Design Provisions for Earthquake Resistance of Structures, Part 1: General Rules, Seismic Actions and Rules for Buildings*, Brussels: European Committee for Standardization.

Calvi, G.M. (2000), "The behaviour of frames infilled with non-reinforced and MURFOR reinforced clay brick masonry walss", Universita Degli Studi Di Pavia dipartımento Di Meccanica Strutturale Laboratorio Materiali e Strutture, Via Abbiategrasso, Italy.

Ghobarah, A., El-Attar, M. and Aly, N.M. (2000), "Evaluation of retrofit strategies for reinforced concrete columns: A case study", *Eng. Struct.*, **22**, 490-501.

Güneyisi, E.M. and Altay, G. (2005), "A study on the seismic behavior of a retrofitted building based on nonlinear static and dynamic analyses", *Earthq. Eng. Eng. Vib.*, **4**(1)**,** 173-180.

Güneyisi, E.M. and Altay, G. (2008), "Seismic fragility assessment of effectiveness of viscous dampers in R/C buildings under scenario earthquakes" *Struct. Safety*, **30**, 461-480.

Han, S.W. and Jee, N.Y. (2005), "Seismic behaviors of columns in ordinary and intermediate moment resisting concrete frames", *Eng. Struct.*, **27**(6), 951-962.

Kara, M.E. and Altin, S. (2006), "Behavior of reinforced concrete rames with reinforced concrete partial infills**",** *ACI Struct. J.*, **103**(5), 701-709.

Karbhari, V.M. (1993), "Strengthening of concrete column stubs through resin infused composite wraps", *J. Thermoplast Compos. Mater.*, **6**, 93-107.

Korkmaz, S.Z., Kamanli, M., Korkmaz, H.H., Donduren, S. and Cogurcu M.T. (2010), "Experimental study on the behaviour of nonductile infilled RC frames strengthened with external mesh reinforcement and plaster composite", *Nat. Haz. Earth Syst. Sci.*, **10**(11), 2305-2316.

Li, J., Samali, B., Ye, L. and Bakoss, S. (2002), "Behaviour of concrete beam–column connections reinforced with hybrid FRP sheet", *Compos. Struct.*, **57**, 357-365.
Massumi, A. and Absalan, M. (2013), "Interaction between bracing system and moment resisting frame in braced RC frames", *Archiv. Civ. Mech. Eng.*, **13**, 260-268.
Nateghi-Alahi, F. (1995), "Seismic strengthening of eight-storey RC apartment building using steel braces", *Eng. Struct.*, **17**(6), 455-461.
Ozcebe, G., Ersoy, U., Tankut, T., Erduran, E., Keskin, O. and Mertol, C. (2003), "Strengthening of brick-infilled RC frames with CFRP", Technical Report, Department of Civil Engineering, Middle East Technical University, Ankara, Turkey.
Ozel, A.E. and Guneyisi, E.M. (2011), "Effects of eccentric steel bracing systems on seismic fragility curves of mid-rise R/C buildings: A case study", *Struct. Safety*, **33**, 82-95.
Pujol, S. and Fick, D. (2010), "The test of a full-scale three-story RC structure with masonry infill walls", *Eng. Struct.*, **32**, 3112-3121.
Smyth, A., Altay, G., Deodatis, G., Erdik, M., Franco, G., Gülkan, P., Kunreuther, H., Luş, H., Mete, E., Seeber, L., and Yüzügüllü, O. (2004), "Probabilistic benefit-cost analysis for earthquake damage mitigation: evaluating measures for apartment houses in Turkey" *Earthq. Spectra*, **20,** 171-203.
Stavridis, A., Koutromanos, I. and Shing, P.B. (2012), "Shake-table tests of a three-story reinforced concrete frame with masonry infill walls", *Earthq. Eng. Struct. Dyn.*, **41**(6),1089-1108.
Susoy, M. (2004), "Seismic strengthening of masonry infilled reinforced concrete frames with precast concrete panels", M.S. Dissertation, Middle East Technical University, Ankara, Turkey.
TEC (2007), *The Ministry of Public Works and Settlement*, *Turkish Code for Buildings in Seismic Zones*, Turkish Seismic Code, Ankara, Turkey.
Uva, G., Porco, F. and Fiore, A. (2012), "Appraisal of masonry infill walls effect in the seismic response of RC framed buildings: A case study", *Eng. Struct.*, **34**, 514-526.

CC